Influence of Excitonic Interactions on the Transient Absorption and Two-Photon Absorption Spectra of Porphyrin J-Aggregates in the NIR Region

ARTICLE *in* THE JOURNAL OF PHYSICAL CHEMISTRY C · DECEMBER 2007

Impact Factor: 4.77 · DOI: 10.1021/jp074974q

3 AUTHORS:

Elisabetta Collini
University of Padova
29 PUBLICATIONS **1,609** CITATIONS
SEE PROFILE

Camilla Ferrante
University of Padova
61 PUBLICATIONS **1,234** CITATIONS
SEE PROFILE

Renato Bozio
University of Padova
169 PUBLICATIONS **3,178** CITATIONS
SEE PROFILE

Influence of Excitonic Interactions on the Transient Absorption and Two-Photon Absorption Spectra of Porphyrin J-Aggregates in the NIR Region

Elisabetta Collini, Camilla Ferrante,* and Renato Bozio

Chemical Sciences Department, University of Padova and INSTM, via Marzolo 1, I-35131 Padova, Italy

Received: June 26, 2007; In Final Form: September 23, 2007

The transient absorption (TA) and two-photon (TPA) absorption spectra of a water-soluble porphyrin, 5,-10,15,20-tetrakis(4-sulfonatophenyl)porphyrin (H_4TPPS^{2-}) diacid, in the monomeric and J-aggregated form are reported. TA spectra, measured with ultrafast laser pulses, were excited at 403 nm and probed at wavelengths varying in the 440−1100 nm range. While the TA spectrum of the J-aggregate form has been already investigated, but only in the 450−750 nm region (Kano, H.; Kobayashi, T. *J. Chem. Phys*. **2002**, *116*, 184), the TA spectrum of the monomer has never been investigated previously. The TPA spectrum, also measured with ultrafast laser pulses in the wavelength range of 380−440 nm, shows an increase of the TPA cross-section per single molecule by a factor of 30 upon aggregation. Even more intriguing is the appearance of a two-photon allowed transition around 410 nm in the TPA and TA spectra of the J-aggregate form, not present either in the TPA or in the TA spectra of the monomer. The physical nature of the two-photon allowed state giving rise to such a band is thoroughly discussed, in relation to the peculiar excitonic properties of molecular aggregates, and it is tentatively attributed to a bi-exciton state.

Introduction

Self-assembled molecular aggregates have always fascinated chemists and physicists because of the spontaneous way in which they form and the peculiar properties they exhibit. Aggregation promotes drastic changes in molecular aggregates' electronic and optical properties. The strong intermolecular coupling between different monomeric units forming the aggregate originates from delocalized excitonic states,[1] which manifest unusual properties such as spectral shift and narrowing of the UV−vis bands[2] and superradiance.[3] Thanks to such properties, these aggregates have been extensively exploited, for example, as photosensitizers in the field of photography.[4] Moreover, aggregates of water-soluble porphyrins are particularly interesting as model systems for the study of photosynthetic processes.[5] A thorough understanding of the exciton delocalization process and the interaction mechanism among the monomer units is a fundamental step in the realization of synthetic antenna devices.

In this context, great effort, both theoretically and experimentally, has been devoted in the last few decades to the description and investigation of molecular interactions giving rise to the peculiar properties of these systems.[6] With respect to their optical properties, these studies came to recognize that the origin of the energy shift observed for the absorption and emission bands with respect to those of the monomer can be well-understood in the frame of excitonic theories.[7,8]

More recently, when experiments of nonlinear optical spectroscopy became feasible, interest in this class of systems was rejuvenated by the many applications that are envisioned in the photonic and optoelectronic fields for these self-assembled systems since they can be endowed with a high nonlinear (NL) optical response and/or high photoconductivity. Transient absorption (TA) as well as photon echo experiments helped in the characterization of the relaxation and dephasing dynamics of the excitonic states from room temperature, down to liquid helium temperature.[9−17] In particular, TA experiments at zero time delay allowed the detection of the two-exciton states predicted by the excitonic theory but not visible in linear absorption spectra.[11,12] These spectra made it possible to estimate the exciton coherence length of the molecular aggregate in solution at room temperature. Also, the exciton lifetime was measured from the time decay of the TA signal, taking care that the pump intensity was suitably attenuated to avoid exciton−exciton annihilation mechanisms. For cyanine, as well as porphyrin aggregates, the exciton lifetime turned out to be approximately 200−400 ps at room temperature.[12,13] Model calculations predict that bi-exciton states may appear in TA experiments at zero time delay as additional bands, falling either at shorter or at longer wavelengths with respect to the one-exciton bleaching, depending on the interaction process giving rise to the bi-exciton formation.[18,19] Up to now, no such band has been observed in the TA spectra of molecular aggregates of cyanines as well as porphyrins, one possible reason being the reduced wavelength range investigated in the TA spectra.

At the same time, theoretical work demonstrated that, under suitable experimental conditions, a net increase of the nonlinear optical response should occur upon aggregation.[20,21] Such an enhancement is often referred to in experimental papers as "a cooperative effect. It should be present when the dephasing rate of the excitonic transition is dominated by pure dephasing and the contribution of the radiative exciton relaxation rate is negligible;[20] therefore, molecular aggregates at room temperature should display an increase in the nonlinear optical (NLO) response.

In this work, we investigated molecular aggregates of the diacid form of water-soluble 5,10,15,20-tetrakis(4-sulfonatophenyl)porphyrin (H_4TPPS^{2-}). The association of many H_4TPPS^{2-} porphyrin units to yield J-aggregates has been detected and thoroughly described by Ohno et al.[22] They observed that, under

* Corresponding author. Tel.: +390498275148; fax: +390498275239; e-mail: camilla.ferrante@unipd.it.

10.1021/jp074974q CCC: $37.00
Published on Web 11/29/2007

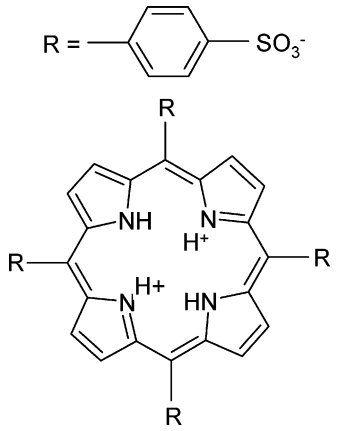

Figure 1. Chemical structure of the diacid form of 5,10,15,20-tetrakis-(4-sulfonatophenyl)porphyrin (H_4TPPS^{2-}).

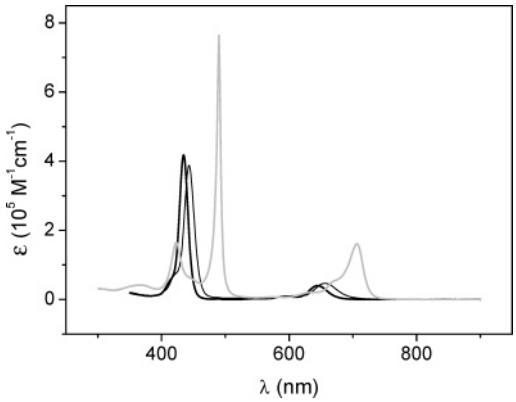

Figure 2. Linear absorption spectra of H_4TPPS^{2-} J-aggregate in acidified water (gray line), H_4TPPS^{2-} monomer in acidified water (thick black line), and H_4TPPS^{2-} monomer in 1:1 water/DMSO mixture (thin black line).

highly acidic conditions (pH $<$ 4), the linear absorption spectrum of solutions with concentrations above 1×10^{-5} M showed the formation of sharp absorption bands at 490 and 706 nm red-shifted with respect to the corresponding monomer bands peaked at 434 and 650 nm, respectively (see Figure 2). Furthermore, the aggregation behavior displays a sensible dependence on the concentration, ionic strength, and pH of the solution.[22] Since then, many experimental papers have been dedicated to the study of structural, photophysical, and optical properties of such systems. Resonance Raman scattering,[23,24] circular dichroism,[25] light scattering techniques,[26] optoacoustic spectroscopy,[27] time-resolved fluorescence, fluorescence up-conversion, and flash photolysis[28,29] have been employed to this aim.

Recently, our group has performed two-photon absorption (TPA) experiments on H_4TPPS^{2-} J-aggregates in water solution at room temperature; the TPA cross-section of the porphyrins in the molecular aggregate turned out to be 30 times larger than the TPA cross-section of the single monomer in the whole spectral range investigated: 380−440 nm.[30,31] Similar experiments have been performed for a cyanine molecule in solution at room temperature, and a net enhancement of the TPA cross-section has been observed in preresonance conditions.[32]

Cooperative enhancement of the TPA response in Zn(II) porphyrin dimers and porphyrin chains has already been observed. These molecular systems differ from the self-assembled aggregates since two or more porphyrin moieties are connected through either a butadyine linker or a metal-to-ligand interaction. Both the ground- and the excited-state properties of these systems are heavily affected by such a linker.[33]

A very intriguing feature appearing in the TPA spectrum of H_4TPPS^{2-} in the aggregate form is a band around 410 nm, whose origin was briefly discussed in our previous work.[30] This two-photon allowed transition can arise from (i) a two-photon allowed state of the H_4TPPS^{2-} monomer whose spectral position does not vary upon aggregation, owing to the fact that transition dipole−dipole coupling, responsible for the exciton bandwidth, is ineffective or weak in the case of two-photon states and (ii) a localized state of the molecular aggregate (bi-exciton or CT state). We can exclude that the state observed at 410 nm belongs to one of the high energy states present in the one-exciton manifold of the B-band and not visible in the linear absorption spectrum. All these states cannot be excited by light, to any appreciable extent even in a linear aggregate, and the oscillator strength concentrates in the transition to the state with the excitation amplitude evenly distributed among the monomers, which is the lowest energy level in J-type aggregates.

A simple comparison with the TPA spectrum of H_4TPPS^{2-} in the monomer form could strike out the first hypothesis, but the bad signal-to-noise ratio affecting the TPA spectrum of the monomer makes it impossible to observe such a feature. To shed light on the nature of the band peaked at 410 nm in the TPA spectrum of the aggregate, TA experiments were carried out and are presented in this paper. For centrosymmetric molecules, such as H_4TPPS^{2-}, these experiments should show transient bands starting from the lowest one-photon allowed excited state of the chromophore (for the porphyrins, the Q-band) and reaching a two-photon allowed higher excited state. Furthermore, the TA technique measures the characteristic decay times for the bands appearing in the TA spectra, and these parameters can be extremely helpful in the attribution of the observed bands. In the case of H_4TPPS^{2-}, we expect that, once the lowest excited electronic state (Q-band state) is populated by the pump pulse and before any possible conformational or other relaxation processes take place, a transient band should appear in the 800−1100 nm region, corresponding to a transition toward the two-photon allowed state, appearing at 410 nm in the aggregate spectrum. The relaxation of this transient feature should follow that of the initially populated Q-band excited state. The TA properties of H_4TPPS^{2-} aggregates in water solution have been investigated in detail by Kobayashi and co-workers[16,17] pumping at either 1.6 eV (775 nm) or 3.1 eV (388 nm) and exploring the spectral range of 440−750 nm with the probe beam. From the time evolution of the TA spectra, the authors attribute a lifetime of ∼300 fs to the higher B-band (490 nm) state and 300 ps to the lowest Q-band state (706 nm). They also observed intra-aggregate vibrational energy redistribution and vibrational cooling occurring on a 4 and 11 ps time scale, respectively. The TA spectrum is dominated, at all the times investigated, by the bleaching of the B- and Q-bands and a strong photoinduced absorption in between them, and no clear evidence of two-exciton or bi-exciton states is observed in such spectra. The present paper differs from their work since (i) the TA spectrum of the monomer is also measured and compared to the TA spectrum of the aggregate and (ii) the TA spectrum of the aggregate is mainly explored in the 800−1100 nm region, where a two-photon allowed state is expected to show up. For the same aggregate, Kobayashi and co-workers also investigated the early time TA spectra with ultrafast time resolution. In these experiments, the TA signals exhibited oscillatory features associated with two molecular vibrational modes falling at 241 and 319 cm^{-1}.[34,35]

Experimental Procedures

5,10,15,20-Tetrakis(4-sulfonatophenyl)porphyrin (TPPS) was purchased from Porphyrin Products, Inc. and employed without further purification.

The J-aggregate form was studied in bidistilled water solutions acidified with HCl (37%) until pH $\approx$ 1 was reached. The analytical concentration[36] C of the aggregate solutions was 1 $\times$ 10^{-3} and 1$-$2 $\times$ 10^{-4} M for the TPA with a white light continuum probe (TPA-WLCP) and the TA experiments, respectively. In both cases, KCl (0.01 M) was added to enhance aggregation. On the other hand, to study the monomeric form of H_4TPPS^{2-}, pump and probe experiments were performed at pH $\approx$ 1, either in water solution at $C = 1 \times 10^{-4}$ M ([KCl] = 0) or in a 1:1 water/DMSO mixture at $C = 1.5 \times 10^{-4}$ M. In the case of TPA-WLCP experiments, because of the different detection limits of the technique, a higher concentration, almost 1×10^{-2} M, is required. Such a concentration is reached in a 1:1 water/DMSO mixture with the addition of urea $\sim$1 g/mL (water/DMSO/urea mixture).

The steady-state absorption spectra of all solutions were collected using a Cary 5 (Varian) UV$-$vis spectrophotometer. The TPA spectra were recorded with the TPA-WLCP method, while the TA measurements were performed with the usual pump and probe technique. Both experiments employed a femtosecond laser source based on a regenerative amplified Ti:sapphire laser system from Spectra Physics, emitting 150 fs long laser pulses at a repetition rate of 1 kHz and centered at 806 nm.

The basic optical setup of these two techniques is quite similar. In both cases, the fundamental laser beam is separated by a 4% beam splitter into two paths: the weaker one generates a WLC and is used as the probe, and the other one is used as a pump pulse.

The main difference between the two experiments resides in the central wavelength employed for the pump pulse, being nonresonant in the TPA-WLCP experiment and resonant for the pump and probe one. For the TPA-WLCP experiment, the pump was set at 812 nm and was directly focused on the sample, while in the pump and probe experiment, it was frequency doubled, using a barium-beta-borate (BBO) doubling crystal, and set at 403 nm. While the pump went through a fixed optical path, the probe passed through a computer controlled motorized delay line that allows a continuous modulation of the delay time Δt between the two pulses from zero up to 1 ns. After the delay line, the probe beam was focused into a sapphire window to generate WLC from 440 to 1100 nm. In both experiments, the WLC still contains a large amount of the fundamental beam at either 812 or 806 nm. To remove this contribution, shortwave or longwave pass filters were suitably employed. The beam waist of the pump beam ($w_{0,pump}$) on the sample can be modulated by means of a 400 mm focal length lens, which was set so that $w_{0,pump} \approx 5w_{0,probe}$. This choice minimizes the effects of possible misalignment of the optical setup and always guarantees a good spatial overlap between the pump and the probe pulses on the sample when the delay line is moved. The pump and probe beams were then focused inside the sample in near-parallel geometry by a spherical mirror. In all experiments, the pump and WLC beams were linearly polarized, and the angle between their polarization vectors was set at approximately 55° (magic angle), to avoid rotational diffusion effects.

In the TPA-WLCP experiment, the sample solution was placed in a 1 mm thick quartz cell, and a repetition rate of 100 Hz was employed to prevent bleaching of the sample. In the pump and probe experiment, instead, the repetition rate was set at 500 Hz for the pump beam and 1 kHz for the probe beam, and the sample was continuously flowed in a 1 mm thick quartz cuvette connected to a micropump, to avoid thermal lensing and photodegradation. After the sample, the pump pulse was blocked, while the probe beam was focused into an optical fiber coupled with a monochromator allowing single wavelength decay measurements. The signal at the selected wavelength was then detected by a photodiode (Si for wavelengths in the visible region and InGaAs in the NIR) and processed differently for the two techniques.

Because of the low repetition rate employed in the TPA-WLCP experiments, the signal was averaged on an oscilloscope and then recorded by the computer, while in the pump and probe experiments, a digital Lock-In amplifier (Stanford Research SR830) was used to average the signal.

It is important to point out that in the TPA-WLCP, the instantaneous absorption of two photons (one from the pump and one from the probe) was detected, avoiding a noticeable excited states population. To this end, the change in the probe transmittance as function of the delay time between pump and probe pulses was measured at a fixed wavelength in a restricted temporal region around $\Delta t = 0$.

Results and Discussion

It is well-known that the diprotonated form of 5,10,15,20-tetrakis(4-sulfonatophenyl)porphyrin (H_4TPPS^{2-}, Figure 1) produces J-type aggregates in a water solution.[22] The formation of J-aggregates is confirmed, in the linear absorption spectrum (Figure 2), by the rise of sharp and intense bands red-shifted (706 and 489 nm) with respect to the diacid monomer's Q- and B-bands (650 and 434 nm, respectively). The aggregate spectrum shows an additional blue-shifted band at 422 nm, in the B-band region, the origin of which is attributed to a symmetry loss of the porphyrin upon aggregation that causes a lift of the 2-fold degeneracy of the two excited electronic energy levels mainly responsible for the B-band.[24] The spectral shape and position of the Q- and B-bands in the absorption spectra of the aggregate do not change in all the solutions investigated in the TPA and TA experiments; therefore, it can be assumed that only one kind of J-type aggregate with a well-defined coherence length is present in all these measurements. Indeed, literature data for H_4TPPS^{2-} aggregates in acidic water solution show that at high analytical concentrations, only a very short and linear J-type aggregate is present in solution.[26]

The absorption bands of the H_4TPPS^{2-} monomer in the acidified water/DMSO mixture with or without urea, and in acidified water at 10^{-5} M, have similar shapes and relative intensities. The only difference is a slight shift of approximately 10 nm toward higher wavelengths in the case of the mixture with respect to water. The absence of aggregate formation in the monomer solutions is confirmed by the fact that, upon dilution, the bands do not change shape or shift in wavelength.

The TPA spectra were recorded by the TPA-WLCP technique, which measures the normalized transmittance of the WLCP caused by a TPA process promoted by one photon of the pump pulse and one photon of the probe itself. The presence of degenerate TPA promoted by the probe or pump beam can be ruled out since the probe intensity is too weak to promote NL effects, and the probe transmittance shows a linear dependence on the pump beam intensity.

In Figure 3, a typical trace for the normalized transmittance of the WLCP as a function of the delay time Δt is reported. At all the investigated probe wavelengths, the signal shows a clear attenuation of the probe beam transmittance at $\Delta t = 0$ (i.e.,

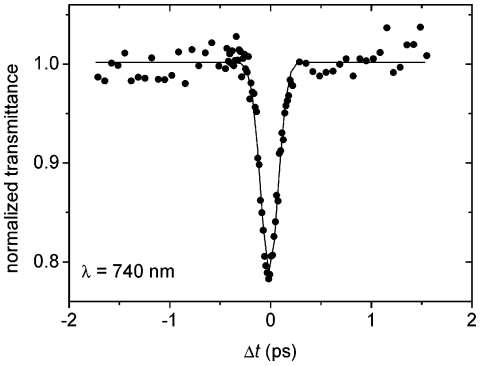

Figure 3. TPA-WLCP trace for $\lambda_{probe} = 740$ nm for a water solution of H_4TPPS^{2-} in the J-aggregate form ($C = 1.15 \times 10^{-3}$ M, pH = ~1, and [KCl] = 0.01 M). Experimental points (full circles) and Gaussian fit (solid line).

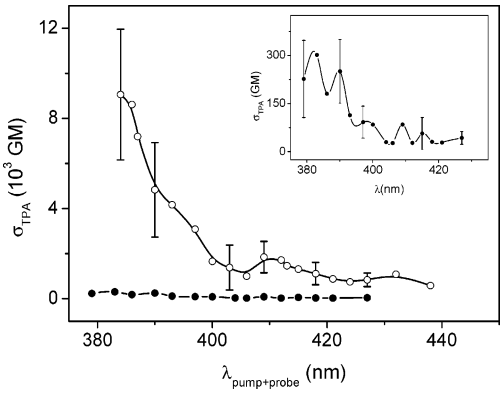

Figure 4. TPA spectra of J-aggregate (open circle) and monomeric diacid form (filled circles) of H_4TPPS^{2-} in solution. Inset shows an enlargement of the monomer TPA spectrum. Full lines are just a guide for the eye. The picture is reprinted from ref 30.

when the pump and the probe beam are overlapped in time), while it maintains the same value before and after the application of the pump pulse. The fwhm of the dip is equal, within experimental error, to the fwhm of the autocorrelation signal for the laser pulses measured with a BBO doubling crystal. From the depth of the dip around $\Delta t = 0$ at the different probe wavelengths, it is possible to extrapolate the two-photon absorption cross-section of the sample under investigation. Details on the analytical procedure are given elsewhere.[30,31,37]

Figure 4 depicts the TPA spectra for the 1.0×10^{-3} M solution of H_4TPPS^{2-} in acid water (open circles) where aggregation occurs and for monomers of H_4TPPS^{2-} in the water/DMSO/urea mixture (full circles), whose enlargement is shown in the inset. On the abscissa scale, the wavelength $\lambda_{pump+probe} = \lambda_{pump}\lambda_{probe}/(\lambda_{pump} + \lambda_{probe})$ is used, where $\lambda_{pump} = 812$ nm. Error bars are estimated from repeated measurements.

The comparison between aggregate and monomer spectra shows clearly that (i) σ_{TPA} increases steeply as $\lambda_{pump+probe}$ decreases in both samples; (ii) σ_{TPA} for the aggregate is strongly enhanced in the whole spectral range investigated; and (iii) there is a band, centered at 410 nm, in the aggregate spectrum. The presence of an analogous band in the monomer spectrum cannot be ascertained because of the poor signal-to-noise ratio. The first two features were explained in terms of one-photon preresonance and cooperative effects; a thorough discussion of these aspects can be found in a previous paper.[30]

The aim of this work was to investigate the nature of the band observed at 410 nm in the aggregate spectrum that can be reasonably attributed to a two-photon resonant state. The nature

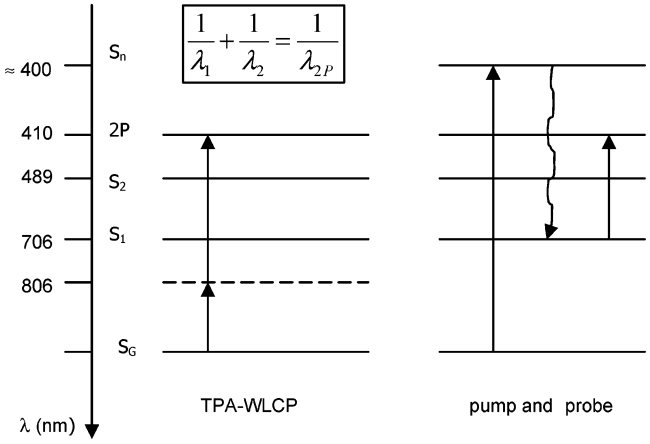

Figure 5. Different pathways for the two-photon absorption process: instantaneous in TPA-WLCP technique and sequential in pump and probe technique. Energy levels for J-aggregate are depicted. The two-photon resonant state found at 410 nm in the aggregate TPA spectrum is indicated by 2P.

of such a state was a source of debate also in a previous paper[30] since it can be (i) a typical state of H_4TPPS^{2-} lying at the same energy in the monomer and the J-aggregate or (ii) a localized state (bi-exciton) of the aggregate. The first hypothesis relies on the fact that for centrosymmetric molecules, such as H_4TPPS^{2-}, two-photon allowed states are characterized by a vanishing transition dipole moment; therefore, it is highly unlikely that they will shift in energy upon aggregation since the exciton transfer energy would also vanish in the dipole approximation. As a consequence, these states should fall at about the same wavelength for the monomer and the aggregate. The second hypothesis is clearly more intriguing in that it would imply an interaction between two excitons in the aggregate, a phenomenon not yet observed in intermolecular aggregates of organic molecules in solution. Bi-exciton states have already been observed in polymers as well as oligomers.[38,39] These systems are quite different from the molecular aggregates analyzed in this paper since the dipolar excitonic coupling among the monomer units is much weaker in our intermolecular aggregate than in intramolecular systems such as oligomers and polymers, in which the monomer units are covalently bound through conjugated covalent bonds. Unfortunately, the TPA spectrum of the monomer was not decisive to reject the first hypothesis since the poor signal-to-noise ratio did not allow one to exclude the presence of a signal at 410 nm.

To fully understand the nature of this band, incoherent pump and probe experiments can be used since this technique has been already exploited successfully to observe excitonic states in J-aggregates.[12,40] The use of pump and probe relies on the idea that, while in the TPA-WLCP experiment the investigated state is reached through instantaneous absorption of two photons without population of any intermediate state, in a pump and probe experiment, the same state should be reached in a sequential pathway, in which the S_1 state (S_1 being the Q-band of the porphyrin either in the monomer or in the J-aggregate form) is populated by the pump beam, and then the two-photon allowed state is reached by absorption of a photon of the probe beam starting from the S_1 state before it relaxes (Figure 5). The S_1 state of H_4TPPS^{2-} falls at 706 and 650 nm in the J-aggregate and monomer, respectively (see Figure 2). Therefore, the wavelength at which an attenuation of the probe beam should occur, after population of the S_1 state, should fall at $\lambda_{probe} =$ ~950 nm and $\lambda_{probe} =$ ~1100 nm in the J-aggregate and monomer, respectively, if the state giving rise to the 410 nm

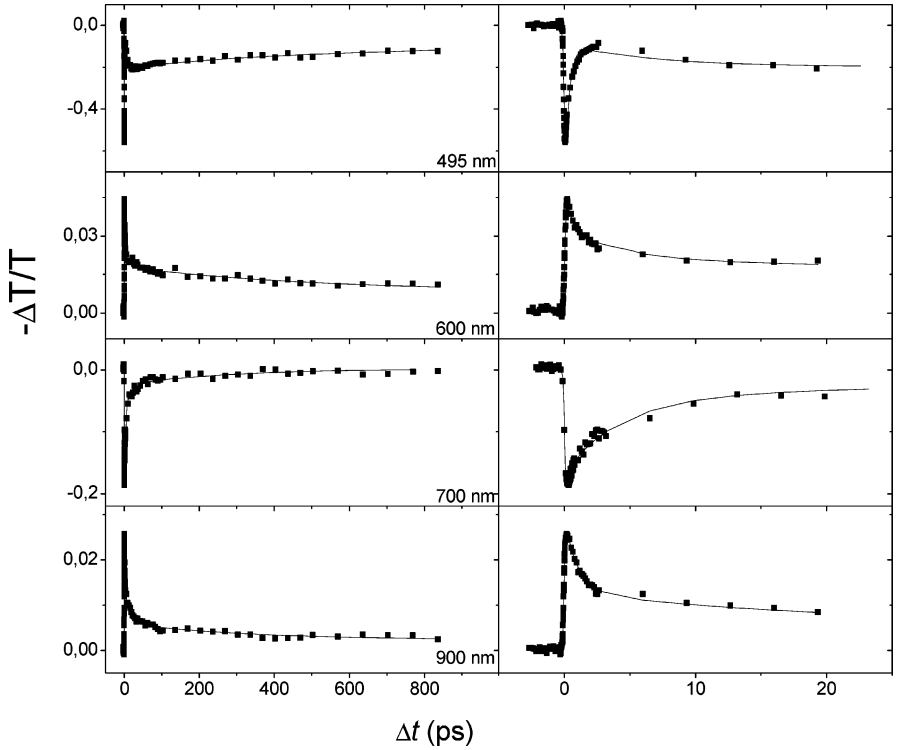

Figure 6. Temporal profiles of the differential transmittance of the probe beam: experimental data points (dots) and corresponding fit (lines) at selected wavelengths for H_4TPPS^{2-} aggregate in water up to 1 ns (left) and 25 ps (right). Negative signal indicates bleaching, while positive signal indicates photoinduced absorption.

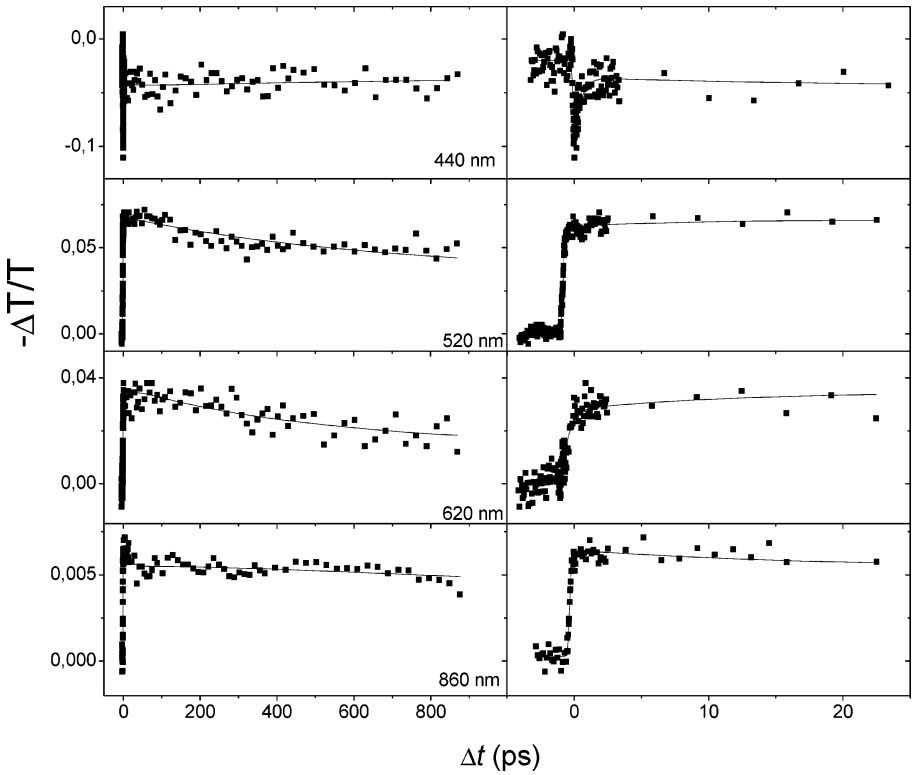

Figure 7. Temporal profiles of differential transmittance of the probe beam: experimental data points (dots) and corresponding fit (lines) at selected wavelengths for H_4TPPS^{2-} monomer in water up to 1 ns (left) and 25 ps (right).

band in the TPA spectrum falls at the same energy for both samples, as supposed by the first hypothesis.

The TA spectra for the aggregate and monomer of H_4TPPS^{2-} were recorded in the 440−1100 nm region, with particular attention paid to the NIR region: 800−1100 nm where the transient peak associated with the investigated state is expected.

Figures 6−8 show the temporal profiles of the probe beam differential transmittance as a function of Δt (dots) and a multiexponential fit of the experimental data (lines) at different probe wavelengths for the J-aggregate solution (Figure 6), the monomer solution in water (Figure 7), and the monomer solution in water/DMSO mixture (Figure 8), respectively.

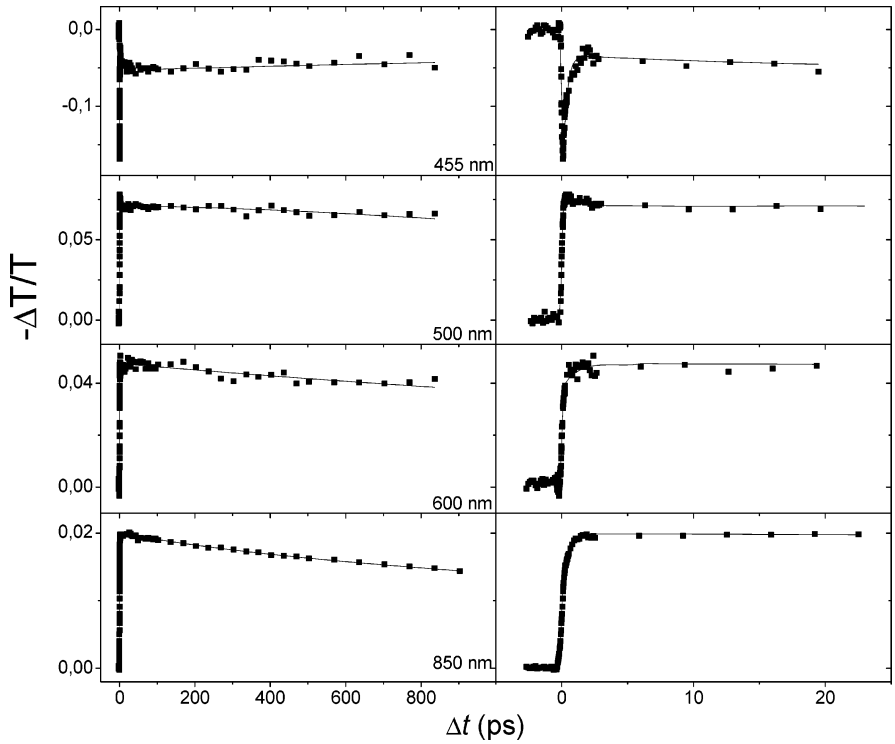

Figure 8. Temporal profiles of differential transmittance of the probe beam: experimental data points (dots) and corresponding fit (lines) at selected wavelengths for H_4TPPS^{2-} monomer in water/DMSO mixture up to 1 ns (left) and 25 ps (right).

For all the samples, the analysis of the decay traces was carried out independently at each wavelength. The fitting program[41] allows deconvolution of the instrument response function from the temporal profile of the molecular response function. A Gaussian function was used to model the instrumental response; its fwhm was fixed to 0.15 ps, the typical value of the pulse duration, as measured by the autocorrelation method. The molecular response function is well-reproduced by a multiexponential function; typically, four terms are necessary to fit the data for the J-aggregate and the diacid monomer both in pure water and in water/DMSO mixture. It is important to bear in mind that the excitation wavelength employed is 403 nm, so that the pump pulse will produce a population directly above the S_2 state (i.e., the state associated with the B-band of H_4TPPS^{2-} both in the J-aggregate and in the monomer form).

The starting value for the characteristic time constants employed to fit the decay curves of the sample in the J-aggregate form were chosen in agreement with the one reported by Kano and Kobayashi in their pioneering work on the characterization of the transient absorption properties of the same aggregates.[17] For the diacid monomer instead, one of the decay time constants was set at 4 ns, the literature value for the lifetime of the S_1 state,[28,29] while the other ones were left free to change.

The TA spectra were derived point-by-point from the fitted data, by plotting the value of the differential transmittance at fixed values of time delay Δt. In all the TA spectra, $-\Delta T/T$ is depicted, so a negative signal corresponds to bleaching, while a positive one corresponds to photoinduced absorption (PIA) from the excited state.

Figure 9 shows the TA spectra for the H_4TPPS^{2-} J-aggregate (a) and an enlargement of the 750−1100 nm region (b), whereas Figure 10 displays the TA spectra for the H_4TPPS^{2-} monomer in water (a) and in the 1:1 water/DMSO mixture (b and c).

Transient Absorption of the Monomer. We first discuss the TA spectra and relaxation dynamics of H_4TPPS^{2-} in the monomer form. The analysis of the decay curves in water suggests that its relaxation dynamics is well-reproduced by the sum of four exponential functions with characteristic time constants: $\tau_1 = 500$ fs, $\tau_2 = 15$ ps, $\tau_3 = 400$ ps, and $\tau_4 \geq 4$ ns (fixed). The physical meaning of each temporal component is evinced through a combined analysis of the TA spectrum and literature data for analogous porphyrins, and they are summarized in Figure 11a with their characteristic time scales.

In the TA spectrum (Figure 10a), after S_2 photoexcitation, bleaching of both transitions to the S_2 and S_1 excited states (B- and Q-bands) around 440 and 650 nm, respectively, is observed. Between them, a broad PIA is also recorded. The latter is a typical feature observed in many porphyrins,[42,43] and it can be associated mainly with excited-state absorption (ESA) from both S_2 and S_1 states up to higher singlet energy states (S_n). A very weak PIA is also present between 750 and 1050 nm. Some authors observed the same feature for similar porphyrins and attribute it either to $S_1 \rightarrow S_n$ transitions or to triplet−triplet excited-state transitions.[42−45] It is well-known that the $S_2 \rightarrow S_1$ internal conversion (IC) in porphyrins is generally very fast (on the order of a few hundreds of femtoseconds),[46,47] so it can be reasonably supposed that the τ_1 component corresponds just to $S_2 \rightarrow S_1$ IC. This fast decay component is present at all wavelengths in the TA spectrum, with a negative amplitude (raising component in the decay curve) where bleaching of S_2 occurs and in almost all the PIA regions. Instead, it shows a positive amplitude just between 600 and 700 nm, indicating that there are excited states S_n that can be reached from S_2 through a one-photon absorption process. Indeed, this transition affects the TA spectrum at $\Delta t = 0$, where the bleaching of S_1 is almost cancelled out by this component, as depicted in Figure 10a.

The intermediate time constants ($\tau_2 = 15$ ps and $\tau_3 = 400$ ps) are also present where PIA occurs, and their amplitudes are small and can be either positive or negative. In particular, the τ_2 component can be assigned to vibrational cooling inside the Q-band since a similar component has been previously observed

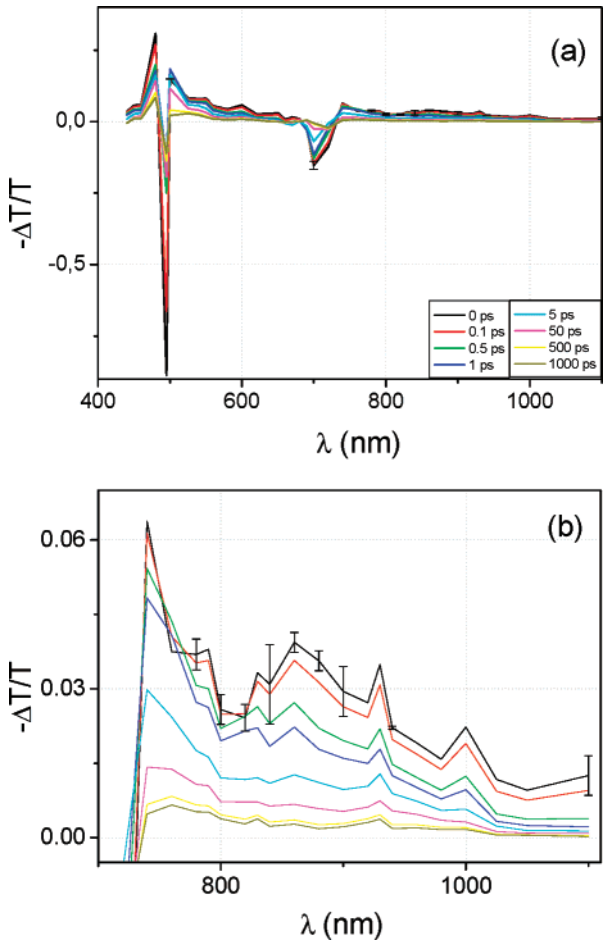

Figure 9. Transient absorption spectra at different delay times for H_4TPPS^{2-} J-aggregate (a) in the whole spectral range investigated (440−1100 nm) and (b) in the NIR region.

in the TA spectra of other porphyrins in solution at room temperature.[46,47]

The longer time (τ_4) used in our model fitting of the decay curves should not be assigned a quantitative meaning because of the limited time window of our measurements. It only mimics the decay dynamics of a comparatively long-lived state such as the fluorescent S_1 state itself or a triplet state (T_1) that can be reached from S_1 through an intersystem crossing (ISC) process. The TA spectrum at long times shows a marked PIA around 460 nm that may be due to transition from S_1 to the same S_n states observed in the TA spectrum of S_2 at early times.

Since the spectral region 800−1050 nm is of key interest for our purposes, the TA measurements in the whole spectral range were repeated in the 1:1 water/DMSO mixture in an attempt at improving the signal-to-noise ratio of the data in water solution. In fact, larger concentrations of monomeric H_4TPPS^{2-} can be attained in this solvent mixture without aggregation. The TA spectrum (Figure 10b) in water/DMSO manifests dynamic properties quite similar to those in water. The characteristic time constants estimated from the fit of the experimental data are τ_1 = 500 fs, τ_2 = 20 ps, τ_3 = 400 ps, and $\tau_4 \geq 4$ ns, similar to those found for the diacid monomer in water, except for the τ_2 time.

As for the data in water, τ_1 is attributed to IC from S_2 to S_1, τ_2 to vibrational cooling inside the Q-band, and τ_4 to the lifetime either of S_1 or T_1. The 400 ps component, instead, appears almost always as a raising component. In the TA spectrum, the growth of a maximum approximately at 850 nm is observed in hundreds of picoseconds, which then lasts well after 1 ns.

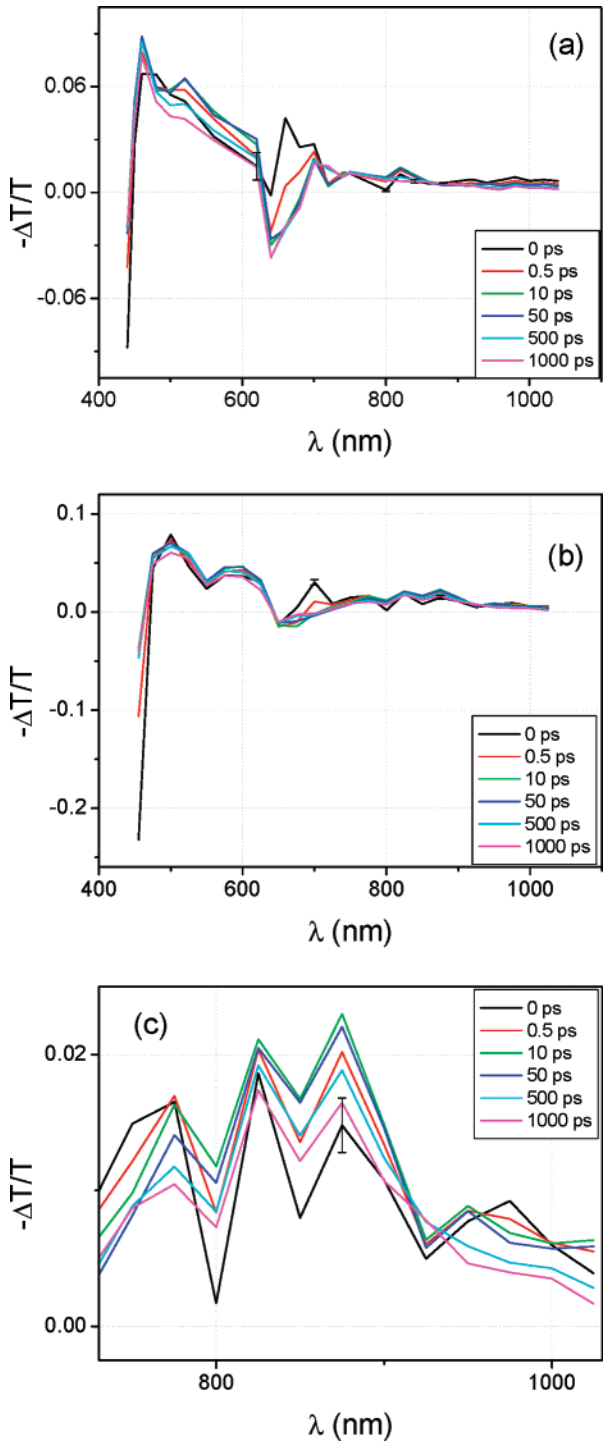

Figure 10. Transient absorption spectra at different delay times for H_4TPPS^{2-} monomer in (a) acidified water and (b) 1:1 water/DMSO mixture. Panel c shows an enlargement of the TA spectra of the monomer in a 1:1 water/DMSO mixture in the NIR region.

Evidence of PIA in this spectral region was reported for similar porphyrins[42−45] and attributed both to $T_1 \rightarrow T_n$ and to $S_1 \rightarrow S_n$ transitions. The available photophysical data for H_4TPPS^{2-} in water,[27,28] however, rule out the assignment to triplet absorption because direct measurements as well as estimates based on the ISC quantum yield and the fluorescence lifetime yield a value of the ISC time in the range of 8−10 ns.

Extensive investigations of the fluorescence dynamics of tetraphenyl-porphyrin (H_4TPP^{2+}) and octaethyl-porphyrin diacid[48] have shown a complex behavior somewhat resembling that of nonplanar highly substituted porphyrins. A biexponential

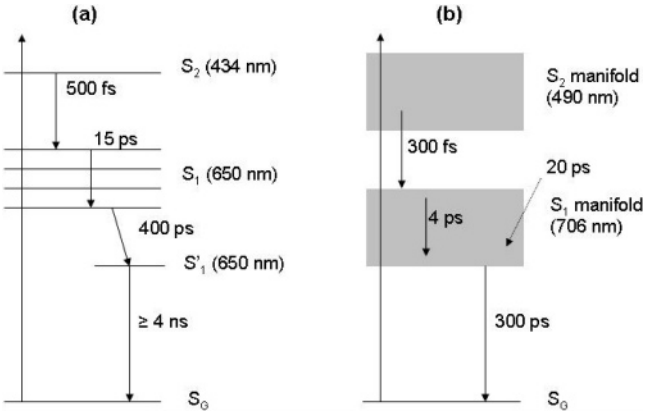

Figure 11. Schematic representation of relaxation processes after photoexcitation for (a) monomer and (b) J-aggregate of H_4TPPS^{2-}. Lines represent single levels, while the gray areas depict energy bands of the aggregate. Arrows represent relaxation processes (see text).

fluorescence decay has been reported for (H_4TPP^{2+}) in toluene with characteristic times $\tau_1 = 480$ ps and $\tau_2 = 1.73$ ns.[48] This dynamics has been interpreted as a result of conformational changes in the excited-state geometry accompanied by an enhancement of the nonradiative decay from the final excited-state conformation. Since the phenomenon appears to be general to a number of diacid substituted porphyrins, it was suggestive to interpret this intermediate decay time in our TA data also as a result of conformational changes.

The amplitude of the exponential component of our model fitting with a 400 ps time constant is negative and small over the spectral range of 700−900 nm. This means that the conformational change brings about only a small intensity enhancement of the TA spectrum without remarkable changes in shape. The observed dynamics of the TA indicates a high degree of conformational flexibility also in H_4TPPS^{2-}.

For the following discussion, it is important to remark that in the TA spectra of H_4TPPS^{2-} at $\lambda_{probe} \geq 1000$ nm, the transient signal is only due to a tail of the PIA centered at 850 nm, and no clear absorption due to a $S_1 \rightarrow S_n$ transition is visible.

Transient Absorption of the Aggregate. Attention is now turned to the TA spectra of the J-aggregate solutions. A first comparison of the aggregate TA spectra (Figures 9), with those of the monomer (Figures 10), immediately shows that the dynamics of the aggregate is much faster than that of the monomer. The faster dynamics is probably due to new nonradiative energy relaxation channels that become effective upon aggregation; this agrees with steady-state and time-resolved fluorescence properties observed by many authors reporting a remarkable decrease of the fluorescence quantum yield and of excited-state lifetime upon aggregation.[29,49] The new nonradiative energy relaxation channels are likely connected with the manifold of states characteristic of the excitonic bands that form upon aggregation. In an ideal cyclic J-aggregate, only the lowest energy state of the one-excition band is one-photon allowed and therefore can be directly populated through optical excitation or give rise to radiative decay. On the other hand, at room temperature after excitation, interactions with the dynamical degrees of freedom can easily populate other states in the excitonic manifold. These states cannot give rise to radiative decay but can provide new fast relaxation channels for the nonradiative decay of the excitation.

The analysis of the excited-state dynamics of J-aggregates relies on the same procedure adopted for the monomer. The decay profiles at each wavelength were fitted by a sum of four exponential functions convoluted with the instrument response function. Around 500−550 nm, the decay curves show also an intense nanosecond long component, which is attributed to residual monomer present in solution. This component is clearly visible in this range, whereas in all the other spectral regions, its contribution is still present but is very small. The TA absorption spectra derived point-by-point from the individual decay curves obtained in the 450−750 nm region (Figure 9a) are in good agreement with those already published by Kano and Kobayashi for the same system,[17] where a thorough discussion of the observed relaxation dynamics is already given. Since our experimental findings confirm the dynamics observed and reported by those authors, in the following, only a brief description of the physical processes associated with them is given. The relaxation dynamics of the H_4TPPS^{2-} aggregates is dominated by four time constants: $\tau_1 = 300$ fs, $\tau_2 = 4$ ps, $\tau_3 = 20$ ps, and $\tau_4 = 300$ ps. The TA spectrum in this region shows many features in common with that of the monomer: two bleaching signals at 700 and 490 nm, relative to the S_2 and S_1 excitonic bands, respectively, and a broad PIA around 550 nm. In contrast to the behavior observed in the monomer, the spectral profile of PIA does not show an initial rising but decreases monotonously with a multiexponential decay containing all four decay time constants. The fast decay ($\tau_1 = 300$ fs) is attributed to IC mainly from S_2 to S_1.[17] Fast IC between the two bands is confirmed by the fact that the fluorescence occurs always from S_1, even if excitation induces population in the S_2 state; furthermore, the S_1 fluorescence lifetime does not change remarkably if the excitation is directed to the S_2 or S_1 band.[49] However, since the bleaching recovery of the S_2 and S_1 band also exhibits the same time constant, this means that part of the population of the S_2 state decays very quickly directly to the ground state. Finally, time-resolved measurements of the $S_2 \rightarrow S_G$ fluorescence, although very weak, also show this time constant.[17,29,34] The nature of the IC process implicitly indicates that hot vibronic states of the S_1 band are instantaneously populated. Following Kano and Kobayashi,[17] the time constants $\tau_2 = 4$ ps and $\tau_3 = 20$ ps are attributed to intra-aggregate and aggregate-solvent vibrational energy redistribution, respectively; the $\tau_4 = 300$ ps component is attributed to S_1 lifetime by comparison with time-resolved fluorescence data.[29] The persistence of the PIA at delay times longer than 20 ps indicates that $S_1 \rightarrow S_n$ processes contribute to this signal.

In the IR region, not investigated previously and where our interest is focused, the aggregate TA spectrum shows two clear PIA peaks centered at 750 and 880 nm. The first PIA feature falls on the red of the J-type excitonic transition of the porphyrin Q-band. Excitation at 403 nm will populate a higher excited state that will decay almost immediately in all the states of the J-exciton Q-band. In the TA spectra, PIA can arise from transitions starting from all the states of the Q-band up to higher excited states of the system (i.e., two-exciton bands or localized bi-exciton states). Two-exciton states are excited states where two, noninteracting, delocalized excitations are simultaneously present in the same aggregate, and they form a band that lies at twice the energy of the one-exciton manifold. Bi-exciton states instead are excited states characterized by the presence of interactions between the two excitations. Depending on the nature (attractive or repulsive) of the interaction, these states will separate from the two-exciton manifold on the low (attractive) or high (repulsive) energy side.[18,19] Numerical simulations[12,40] have shown that a blue-shifted PIA should be observed for transitions from any state of the one-exciton manifold toward the two-exciton one, whereas a red-shifted PIA would result from transitions involving a bi-exciton state

characterized by attractive interactions. Because the PIA observed experimentally is red-shifted, it could be a signature of a bi-exciton state. On the other hand, the TA spectrum of the diacid monomer shows a maximum around 850 nm, due to a transition toward a two-photon allowed state. This same state can be responsible for the PIA at 750 nm in the aggregate since, as shown in Figure 2, the S_1 exciton state falls at 706 nm, and it needs another 750 nm jump to reach the same spectral region that in the monomer can be reached after population of the Q-state at 650 nm followed by absorption at 850 nm. Indeed, the energy of the two-photon allowed states of the diacid porphyrin should not be affected by the aggregation process since they have a vanishingly small transition dipole moment.

The dynamics of the 820−950 nm PIA region exhibits both instantaneous ESA from hot S_1 exciton manifold to higher excited states of the aggregate, with time constants of 4 and 20 ps, and ESA from the vibrationally relaxed S_1 manifold, which lasts for a time equal to the S_1 lifetime (300 ps). Because of the fast decay time of this component and the low triplet quantum yield of H_4TPPS^{2-} in the aggregated form, it is possible to exclude triplet−triplet excited-state absorption that usually occurs in this spectral region. The presence of this band confirms the existence of a two-photon allowed excited state falling around 390−405 nm for the H_4TPPS^{2-} aggregate and is almost in the same spectral region where the 410 nm maximum of the TPA spectrum is observed. One reason for the spectral shift observed for this transition can reside in the different excitation pathway employed in the two techniques: simultaneous for the TPA spectrum (in TPA-WLCP, the two photons are absorbed at the same time) and sequential in the TA experiment since the pump beam populates a higher excited state. The sequential absorption implies a redistribution of population within the Q-exciton band, likely with a 4 ps intermediate decay time. Thus, the transient absorption actually starts from a distribution of exciton states that partially maps the exciton bandwidth of about 2000 cm^{-1}. Furthermore, if the final state is a localized bi-exciton state, motional narrowing of the vibronic structure is not effective anymore, and one- and two-photon absorption processes may exhibit different vibronic structures.

A comparison of the PIA observed in the TA spectra of H_4TPPS^{2-} in the 800−1050 nm region for the monomer in the water/DMSO mixture and for the aggregate in water allows us to ascertain if the two-photon allowed state falling at 390−405 nm is an excitonic state present only in the aggregate or a molecular state, which is not influenced by excitonic interactions. In this spectral region, the monomer shows just a weak PIA centered at 850 nm and a vanishingly small PIA at $\lambda_{probe} \geq 1000$ nm. The aggregate spectrum, instead, shows a clear band at the expected wavelength. It is then reasonable to consider this spectral feature as the result of an excitonic driven state of the aggregate, whose nature is now discussed.

The observed state could be attributed to a bi-exciton state arising from the two-exciton manifold because of attractive interactions between two excitons. The interaction between the two excitations is usually described through a multipolar expansion that at the lowest order is just related to the change in the permanent dipole moment of the monomer molecule upon excitation.[50] Following the description given by Knoester and Spano in ref 40, and estimating the nearest neighbor interaction energy J to be approximately -600 cm^{-1} (0.075 eV) from the aggregate absorption spectrum, there must be a change in the permanent dipole moment of H_4TPPS^{2-} of the order of 10−20 D. This is exceedingly larger than the dipole moment difference estimated by Ogawa et al.[51] for porphyrin J-aggregates from electroabsorption measurements.

On the other hand, bi-exciton states may be stabilized, with respect to two-exciton states, by other types of interactions between neighboring electronically excited molecules. These may include polarization, dispersion, and charge transfer interactions under the condition that two neighboring excited molecules interact more strongly than two excited molecules surrounded by ground-state ones. A more formal way to express this simple idea has been put forward in a recent theory proposed by Juzeliunas and Reineker[52] whereby the attractive interaction between excitons is mediated and amplified by the presence of higher molecular levels. Charge transfer states, beside molecular ones, can also contribute to such a mechanism.

In previous papers,[38,39] the presence of bi-exciton states in oligomers and polymers was detected from pump power dependent TA spectra showing the appearance of a fast decaying component whose amplitude is power dependent. Since we do not pump directly in the Q-exciton band, the decay observed shows also the fast internal conversion form the B-exciton band to the Q-exciton band. The presence of this fast decay component is likely to mask the possible presence of a fast decay component arising from the population and relaxation of the bi-exciton state. Kobayashi and co-workers[16,17] performed pump power dependent TA experiments pumping at 1.6 eV, just below the Q-exciton band. Although they observed a fast decay, whose amplitude increases as the pump power increases, they question its attribution to bi-exciton formation. It is important to point out that pumping at this wavelength will not excite directly the bi-exciton state we observe because the photon energy is too high for a direct two-photon absorption.

A realistic assessment of these possibilities and a final attribution could be made only with additional experiments clarifying the nature of the state or theoretical calculations that can predict the spectral position of the two-photon allowed states in the monomer H_4TPPS^{2-} and the energy at which the two-exciton and bi-exciton states of the aggregate should fall.

Conclusion

The TPA and TA spectra of H_4TPPS^{2-} in both monomer and J-aggregate form in aqueous solution are presented. This is the first time, to our knowledge, that the TA spectrum of the monomer was observed. The relaxation dynamics of H_4TPPS^{2-} in the 1:1 water/DMSO mixture is characterized by a 500 fs fast component due to S_2 to S_1 internal conversion, a 40 ps component attributed to vibrational cooling, a 300 ps component recognized as a conformational rearrangement in the S_1 excited state, and a long component ($\geq$4 ns) attributed to the S_1 state lifetime.

The most salient features observed in the comparison of the monomer and aggregate TA and TPA spectra are (i) a faster dynamics of the aggregate with respect to the one of the monomer and (ii) a two-photon allowed state falling at 390−410 nm, whose absorption band is visible in the TPA and TA spectra of the aggregate and not in the ones of the monomer.

The first feature is associated with new nonradiative energy relaxation channels that become effective upon aggregation. The second feature (i.e., the appearance of the 390−410 nm state solely in the TPA and TA spectra of the aggregate) is discussed, and it is argued that this experimental evidence is consistent with the existence of a bi-exciton state in the molecular aggregates. Since the monomer molecules are characterized by a vanishingly small permanent dipole moment, the interactions giving rise to the bi-exciton state cannot be the conventional

electrostatic ones but may include polarization, dispersion, and charge transfer interactions under the condition that two neighboring excited molecules interact more strongly than two excited molecules surrounded by ground-state ones.

Acknowledgment. We are especially grateful to Dr. Rick S. Francis for the gift of the RFGraph program, used to fit the experimental data. This work was supported by Grants FIRB RBNE01P4JF and RBNE033KMA, PRIN2004 n.2004033197, and PRIN2006 n. 2006031511 from the Italian Ministry of Education and Research (MIUR) and PRISMA2005 from Consorzio I.N.S.T.M.

Supporting Information Available: Enlargment of two-photon absorption spectrum of aggregate around 410 nm band. This material is available free of charge via the Internet at http://pubs.acs.org.

References and Notes

(1) Kuhn, H.; Kuhn, C. Chromophore coupling effects. In *J-Aggregates*; Kobayashi, T., Ed.; World Scientific: Singapore, 1996; p 1.
(2) Didraga, C.; Knoester, J. *Chem. Phys.* **2002**, *275*, 307.
(3) de Boer, S.; Vink, K. J.; Wiersma, D. A. *Chem. Phys. Lett*. **1987**, *137*, 99.
(4) Tani, T. Fermions on a Frenkel Chain: Nonlinear Optical Response of Linear Aggregates. In *J-Aggregates*; Kobayashi, T., Ed.; World Scientific: Singapore, 1996; p 209.
(5) Van Amerongen, H.; Valkunas, L.; van Grondelle, R. *Photosynthetic Exitons*; World Scientific: Singapore, 2000.
(6) Kobayashi, T., Ed. *J-Aggregates*; World Scientific: Singapore, 1996 and references therein.
(7) Davydov, A. S. *Theory of Molecular Excitons*; Plenum Press: New York, 1971.
(8) Sturge, M. D. Introduction. In *Excitons*; Rashba, E. I., Sturge M. D., Eds.; North-Holland: Amsterdam, 1982; p 1.
(9) Fidder, H.; Terpstra, J.; Wiersma, D. A. *J. Chem. Phys.* **1991**, *94*, 6895.
(10) Fidder, H.; Knoester, J.; Wiersma, D. A. *J. Chem. Phys*. **1991**, *95*, 6564.
(11) Durrant, J. R.; Knoester, J.; Wiersma, D. A. *Chem. Phys. Lett.* **1994**, *222*, 450.
(12) van Brugel, M.; Wiersma, D. A.; Duppen, K. *J. Chem. Phys*. **1995**, *102*, 20.
(13) Ohta, K.; Yang, M.; Fleming, G. R. *J. Chem. Phys*. **2001**, *115*, 7609.
(14) Lee, J. H.; Min, C. K.; Joo, T. J. *Chem. Phys*. **2001**, *114*, 377.
(15) Brixner, T.; Stenger, J.; Vaswani, H. M.; Cho, M.; Blankenship, R. E.; Fleming, G. R. *Nature (London, U.K.)* **2005**, *434*, 625.
(16) Misawa, K.; Kobayashi, T. *J. Chem. Phys*. **1999**, *110*, 5844.
(17) Kano, H.; Kobayashi, T. *J. Chem. Phys.* **2002**, *116*, 184.
(18) Spano, F. C.; Manas, E. S. *J. Chem. Phys.* **1995**, *103*, 5939.
(19) Ezaki, H.; Tokihiro, T.; Hanamura, E. *Phys. Rev. B: Condens. Matter Mater. Phys.* **1994**, *50*, 10506.
(20) Spano, F. C.; Knoester, J. J-Aggregates in spectral sensitization of photographic materials. In *Advances in Magnetic and Optical Resonance*; Warren, W. S., Ed.; Academic Press: New York, 1994; p 117 and references therein.
(21) Spano, F. C.; Mukamel, S. *J. Chem. Phys*. **1991**, *95*, 7526.
(22) Ohno, O.; Kaizu, Y.; Kobayashi, H. *J. Chem. Phys*. **1993**, *99*, 4128.
(23) (a) Akins, D. L.; Zhu, H.-R.; Guo, C. *J. Phys. Chem*. **1994**, *98*, 3612. (b) Akins, D. L.; Zhu, H.-R.; Guo, C. *J. Phys. Chem*. **1996**, *100*, 5420.
(24) Chen, D. M.; He, T.; Cong, D. F.; Zhang, Y. H.; Liu, F. C. *J. Phys. Chem. A* **2001**, *105*, 3981.
(25) Ribò, J. M.; Crusats, J.; Saguès, F.; Claret, J.; Rubires, R. *Science (Washington, DC, U.S.)* **2001**, *292*, 2063.
(26) (a) Micali, N.; Villari, V.; Castriciano, M. A.; Romeo, A.; Scolaro, L. M. *J. Phys. Chem. B* **2006**, *110*, 8289. (b) Micali, N.; Villari, V.; Scolaro, L. M.; Romeo, A.; Castriciano, M. A. *Phys. Rev. E: Stat., Nonlinear, Soft Matter Phys.* **2005**, *72*, 50401.
(27) Gensch, T.; Viappiani, C.; Braslavsky, S. E. *J. Am. Chem. Soc*. **1999**, *121*, 10573.
(28) Goncalves, P. J.; Aggarwal, L. P. F.; Marquezin, C. A.; Ito, A. S.; de Boni, L.; Barbosa Neto, N. M.; Rodriguez, J. J.; Zilio, S. C.; Borissevitch, I. E. *J. Photochem. Photobiol., A* **2006**, *181*, 378.
(29) Miura, A.; Shibata, Y.; Chosrowjan, H.; Mataga, N.; Tamai, N. *J. Photochem. Photobiol., A* **2006**, *178*, 192.
(30) Collini, E.; Ferrante, C.; Bozio, R. *J. Phys. Chem. B* **2005**, *109*, 2.
(31) Collini, E.; Ferrante, C.; Bozio, R. *Mater. Res. Soc. Symp. Proc.* **2005**, *846*, 39.
(32) Belfield, K. D.; Bondar, M. V.; Hernandez, F. E.; Przhonska, O. V.; Yao, S. *Chem. Phys*. **2006**, *320*, 118.
(33) (a) Ogawa, K.; Kobuke, Y. *J. Photochem. Photobiol., C* **2006**, *7*, 1. (b) Drobizhev, M.; Stepanenko, Y.; Dzenis, Y.; Karotki, A.; Rebane, A.; Taylor, P. N.; Anderson, H. L. *J. Phys. Chem. B* **2005**, *109*, 7223.
(34) Kano, H.; Kobayashi, T. *J. Lumin.* **2002**, *100*, 269.
(35) Kano, H.; Saito, T.; Kobayashi, T. *J. Phys. Chem. A* **2002**, *106*, 3445.
(36) Analytical concentration describes the concentration of monomer molecules used to prepare the solutions and is calculated from the weighted amount of porphyrins and volume of the solution prepared.
(37) Negres, R. A.; Hales, J. M.; Kobyakov, A.; Hagan, D. J.; Van Stryland, E. W. *IEEE J. Quantum Electron.* **2002**, *38*, 1205.
(38) Klimov, V.; McBranch, D. W.; Barashkov, N.; Ferraris, J. *Phys. Rev. B: Condens. Matter Mater. Phys.* **1998**, *58*, 7654.
(39) Klein, G.; Jundt, C.; Sipp, B.; Villaeys, A. A.; Boeglin, A.; Yassar, A.; Horowitz, G.; Garnier, F. *Chem. Phys.* **1997**, *215*, 131.
(40) Knoester, J.; Spano, F. C. Theory of Pump-Probe Spectroscopy of Molecular J-Aggregates. In *J-Aggregates*; Kobayashi, T., Ed.; World Scientific: Singapore, 1996; p 111.
(41) Francis, R. S. *RFGraph*; shareware program http://www.xray.cz/ecm-cd/soft/win/index0065.html.
(42) Rodriguez, J.; Kirmaier, C.; Holten, D. *J. Am. Chem. Soc*. **1989**, *111*, 6500.
(43) O'Keefe, G. E.; Denton, G. J.; Harvey, E. J.; Phillips, R. T.; Friend, R. H.; Anderson, H. L. *J. Chem. Phys*. **1996**, *104*, 805.
(44) Kalyanasundaram, K.; Neumann-Spallart, M. *J. Phys. Chem*. **1982**, *86*, 5163.
(45) Gratz, H.; Penzkofer, A. *Chem. Phys*. **2000**, *254*, 363.
(46) Baskin, J. S.; Yu, H. Z.; Zewail, A. H. *J. Phys. Chem. A* **2002**, *106*, 9837.
(47) Baskin, J. S.; Yu, H. Z.; Zewail, A. H. *J. Phys. Chem. A* **2002**, *106*, 9845.
(48) Chirvony, V. S.; van Hoek, A.; Galievsky, V. A.; Sazanovich, I. V.; Schaafsma, T. J.; Holten, D. *J. Phys. Chem. B* **2000**, *104*, 9909.
(49) Akins, D. L.; Ozcelik, S.; Zhu, H. R.; Guo, C. *J. Phys. Chem*. **1996**, *100*, 14390.
(50) Agranovich, V. M.; Galanin, M. D. *Electronic Excitation Energy Transfer in Condensed Matter, Modern Problems in Condensed Matter Science*; Agranovich, V. M., Maradudin, A. A., Eds.; North Holland Publishing Company: Amsterdam, 1982.
(51) Ogawa, T.; Tokunaga, E.; Kobayashi, T. *Chem. Phys. Lett*. **2005**, *410*, 18.
(52) Juzeliunas, G.; Reineker, P. *J. Chem. Phys.* **1998**, *109*, 6916.